

Available online at www.sciencedirect.com

ScienceDirect

Procedia Computer Science 60 (2015) 808 – 817

Procedia
Computer Science

19th International Conference on Knowledge Based and Intelligent Information and Engineering Systems

A Framework of MRI Fat Suppressed Imaging Fusion System for Femur Abnormality Analysis

Belinda Chong Chiew Meng^{abcd}, Umi Kalthum Ngah^a, Bee Ee Khoo^a, Ibrahim Lutfi Shuaib^b, Mohd Ezane Aziz^c^aSchool of Electrical and Electronic Engineering, Universiti Sains Malaysia, 14300 Nibong Tebal, Malaysia^bAdvanced Medical and Dental Institute, Universiti Sains Malaysia, 13200 Kepala Batas, Malaysia^cDepartment of Radiology, Health Campus, Universiti Sains Malaysia, 16150 Kubang Kerian, Malaysia^dFaculty of Electrical Engineering, Universiti Teknologi MARA (Penang), 13500 Permatang Pauh, Malaysia

Abstract

Short T1 Inversion Recovery (STIR) is a fat suppressed technique commonly used in Magnetic Resonance Imaging (MRI) to suppress fat signals from tissues. The technique is to improve visual inspection during diagnosis. Suspected fluids will appear bright in STIR to identify the abnormality. Due to hardware limitation, tissue contrast and signal-to-noise ratio are reduced. We propose a framework of image fusion system which mimics the MRI machine to produce a fused 'STIR' image. The resultant fused 'STIR' image has high similarity index (0.989971), small mean square error (0.1092), high peak signal-to-noise ratio (106.9173) and good Pearson correlation coefficient (0.696).

© 2015 The Authors. Published by Elsevier B.V. This is an open access article under the CC BY-NC-ND license (<http://creativecommons.org/licenses/by-nc-nd/4.0/>).

Peer-review under responsibility of KES International

Keywords: MRI, fat suppressed imaging, STIR, image fusion, SNR

1. Introduction

MRI scans are non-invasive modern imaging techniques. It provides detailed diagnostic images of most of the important organs and tissues of the body. Because of this, it is an important tool to help medical experts in investigating the causes of diseases.

*Corresponding author.

E-mail address: belinda.chong@ppinang.uitm.edu.my (B. Chong), eeumi@usm.my (Ngah. U.K.), beekhoo@usm.my (BE Khoo), ibrahim@amdi.usm.edu.my (I.L. Shuaib), drezane@kb.usm.my (M.E. Aziz)

MRI allows the suppression of fat or water signals for the enhancement of the suspected tissues for diagnostic purposes. Fat suppressed imaging is one of the commonly used techniques in MRI. Short T1 Inversion Recovery (STIR) is an inversion recovery sequence whereby the value of inversion time is chosen so that the fat signal does not contribute to the resulting image. Clinically, STIR images are useful as the fat signal is suppressed and the contrast of abnormal fluid is enhanced making it easier to identify the appearance of pathological characteristic.

Inversion recovery is an important pulse sequence. Pulse sequence is a preselected set of defined radio frequency and gradient pulses. During the process of scanning, the pulse sequence is repeated to form the MRI images. Two scan parameters need to be controlled to produce the desired pulse sequences i.e, the repetition time (TR) and echo time (TE). To produce STIR images, the sequences are used to give heavy T1-weighting image to demonstrate good contrast between tissues. T1 contrast will be inverted to suppress the fat tissues. TE is then increased to enhance the contrast between tissues [1, 2]. These processes enhance the tumour appearance.

Unfortunately, STIR sequence has the drawback of low signal to noise ratio (SNR). SNR is the difference in signal intensity between the area of interest and the background. The low SNR is often due to magnetic field strength and coil selection. The low SNR affects human visibility to perceive low contrast structures [3]. Therefore, extra care is needed to interpret the sequence. This is because all lesions are crucial, they are not to be missed and noise should not be overly interpreted as a lesion [4, 5].

In addition, MRI scanning process required lengthy acquisition time. It can be up to 90 minutes or more depending on the number of weighted images required. Patients are required to be still during the scanning process. Besides, MRI machine will create hammering noises. This will cause discomfort to patients, resulting in movements which produce poor quality images.

2. Literature review

During diagnoses, high SNR is desirable to investigate the histologic types and location of tumours. Generally, SNR can be improved by increasing the TE scan parameter [5]. SNR can be increased by increasing the TE but it is available only for T1 sequences. Besides TE parameter setting, field of view (FOV) setting can improve SNR [6]. However, different patients may need different setting. It often depends on the size of the patient and location of the disease. FOV setting affects the quality of the image. [7] If the field of view is set too large, relative to the patient or if the scanning distance is not at an isocenter position then there is a risk of inhomogeneity appearance on the image. Inhomogeneity is one of the artifacts which causes shading effects to appear on the image and produces images of poor quality [8].

Increasing slice thickness is another method to increase SNR [6]. This is because the thicker slices are associated with less noise [9] [10]. Unfortunately, thin slices with high SNR are often desirable. This is because thinner slice contain more signal information about a patient. Besides, SNR and image resolution can be improved by decreasing the size of the image. However, decreasing the size of the image is not a good idea because it will affect human visibility. Some other common factors which could affect SNR are field strength [6], coil selection, patient positioning and motion. These factors could cause blurring, reduce resolution and may also generate artifacts.

In 1992, Guido et al. [11] applied the anisotropic diffusion method to improve spatial resolution and they are able to maintain sufficient SNR for visual evaluation. The filtered method obtained good quality image for high field MR imaging but is unsatisfactory for a lower field MR imaging.

Takahara et al. [12] used diffusion-weighted whole-body imaging (DWI) with background body signal suppression (DWIBS) to increase the SNR. Tomoaki et al. [13] then hypothesized that high-b-value DW-MRI could be used to improve the tumour detection. The study is to evaluate the usefulness of high-b-value DW-MRI in the detection of colorectal adenocarcinoma and pancreatic adenocarcinoma [14]. The technique is speedy and requires no contrast agent. Unfortunately, both study populations are small therefore the results need to be confirmed in larger clinical studies.

Oner et. Al [15] used a method known as parallel imaging that use spatial sensitivity information of multiple receiver surface coil to partially replace spatial encoding. The method improves the SNR of single breath-hold DWI of the liver without compromising apparent diffusion coefficient (ADC).

Super-resolution (SR) techniques have been applied into MRI data early 2000s. In 2002, Greenspan et al. [16] proposed a super-resolution method for MRI reconstruction to improve spatial resolution. They used an interactive super-resolution algorithm of data sets to improve resolution. The method improved visualization and SNR

efficiency of the data acquisition. E. Plenge et al. used SR reconstruction methods which are based on iterative back-projection, algebraic reconstruction and regularized least-square to improve resolution, SNR and acquisition time trade-offs. In 2013, D. H. Poot [10] applied SR method for diffusion weighted imaging to enhance the spatial resolution of diffusion tensor data. It shows that SR method is useful for MRI reconstruction that could improve spatial resolution and SNR.

Nuclear magnetic resonance (NMR) spectroscopy has become an important technique for determining the structure of organic compounds over past fifty years. ^{19}F MRI is one of the improved technology of NMR image formation. It is a rare procedure because of the negligible occurrence of fluorine in biological samples [17]. However, ^{19}F resonance is suited for NMR imaging which is used for cancer detection. It allows direct detection of labelled cells for unambiguous identification and quantification [18]. Florian et al. [19] used a method known as paramagnetic relaxation enhancement to improve SNR efficient in ^{19}F MRI. A standard GE sequence and an ultrafast radial sequence are used to increase SNR efficiency. The comparison was done between non paramagnetic compounds and paramagnetic compounds, which shows that paramagnetic compounds has good results with T1 in the range of 1-5 ms. The method can be further improved with signal enhancement which lowers the ^{19}F detection limit.

Obviously, to obtain a good quality image, it often depends on MRI radiographer setting and hardware condition of the machine. In mid-1980s, diffusion MRI method came into existence [20]. The method provided the mapping of the diffusion process of molecules especially in biological tissues. Guido et al., Takahara et al., Tomoaki et al and Oner et. Al. used different types of diffusion methods. In order to obtain good quality image, the method need high power magnetic field for the diffusion process. It increases the cost because of high magnetic power of MRI. SR methods could improve resolution and SNR. There are researchers such as Greenspan et al., E. Plenge et al. and D. H. Poot et al. who used super-resolution algorithms for reconstruction. This method often needs more robust scanning sequence to avoid artifact. Besides, good quality image reconstruction require more slices from different angles and direction. These increase the scanning time.

Medical image fusion is the process of integrating relevant information from multiple images to improve the imaging quality. The produced medical images could increase the clinical applicability for diagnosis. In this study, we proposed a fused image which is the integration of the T1 and T2 sequence that produces 'STIR' like or other fat suppressed images. This could increase the assessment of medical problems. The produced 'STIR' like image has higher SNR if compared to the MRI STIR. The image fusion system imitates the MRI machine during the STIR image acquisition where the contrast of T1 will be reversed in addition to the contrast of T2. The resultant fused image could effectively remove fat tissue from the image. It is important for the expert in interpreting the image. Another advantage is that it does not require long acquisition time and has higher SNR than the STIR image. The fused image could become an alternative for MRI sequence which could provide extra information on STIR to improve diagnostic reading.

3. Framework of Image Fusion System

The image fusion system imitates the MRI machine to produce the fused 'STIR' image. It is based on the inverse contrast of T1 and the additional contrast of T2. The process will cause the fat signal to be removed and water intensity to be enhanced [4]. The image fusion system integrates T1 and T2 sequence and form the fused 'STIR' image. The framework of the image fusion system is summarized in Fig. 1.

First, the image fusion reads T1 and T2 from the original MRI data images. To suppress the fat signal in T1 weighted image, T1 image will be first pre-processed (Fig. 2(a)) and the region of interest (ROI) will be defined as shown in Fig. 2(b).

Fig. 2(c) shows the histogram of the ROI in T1. The histogram shows that fat signal has high intensity. Thresholding is one of the powerful methods of image segmentation which can separate object from background. In this study, basic global threshold is used to compute the threshold value by averaging the intensity values of m_1 (low intensity value) and m_2 (high intensity value) for the pixels between muscle (with or without tumour) and fat. A binary image will be produced based on the threshold value calculated by using Equation 1 [21] to separate the fat signal tissue from the muscle and tumour.

$$T = \frac{1}{2}(m_1 + m_2) \quad (1)$$

where m_1 is the low intensity values of muscle and tumour; m_2 is the high intensity values of fat.

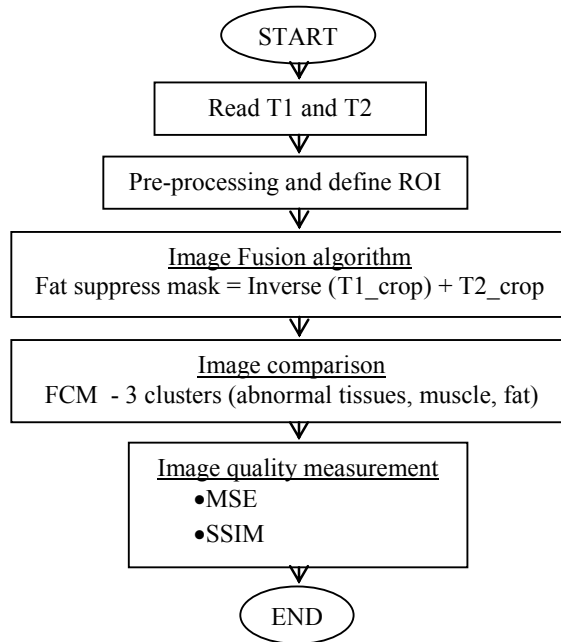


Fig. 1 Framework of image fusion system

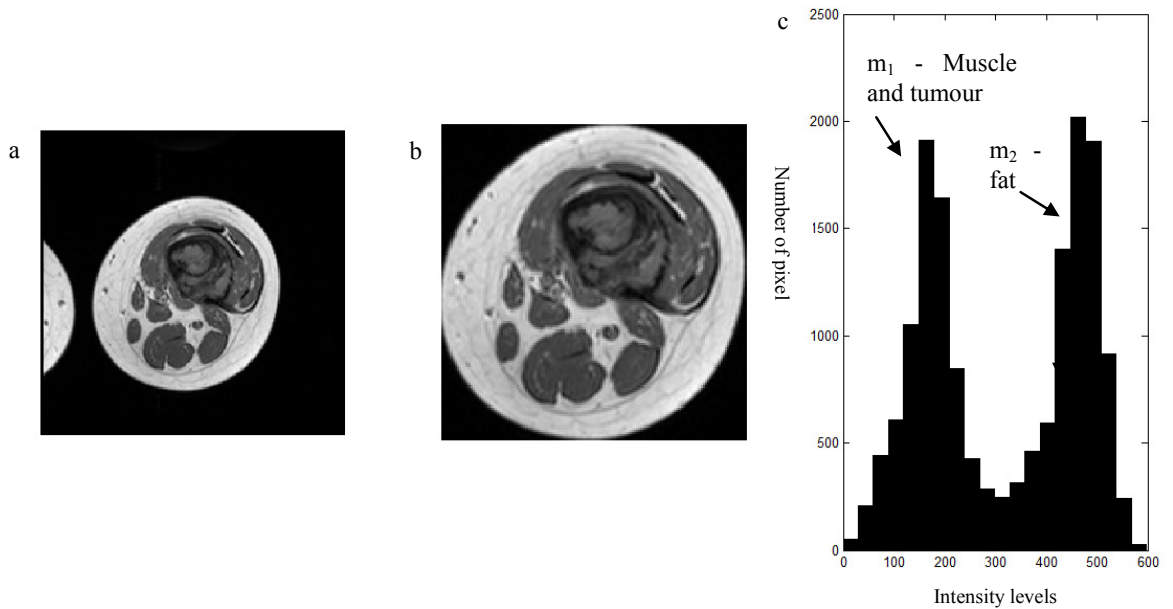


Fig. 2 (a) Original T1 image; (b) Region of interest T1; (c) Histogram of T1

To produce STIR image on MRI machine, sequences used to give heavy T1-weighting image to demonstrate good contrast between tissues. The T1 image will then be inverted to suppress the fat tissue. Based on this concept, the image fusion system obtains the binary T1 image then inverse the T1 image to suppress the fat tissue. The binary T1 image output is shown in Fig. 3(a). The white regions are the fat signals on T1 which need to be inverted. A fat suppressing mask which is the inverse of binary output would remove the fat signal on T1 as shown in Fig. 3(b). This process mimicks the MRI machine to suppress the fat tissue.

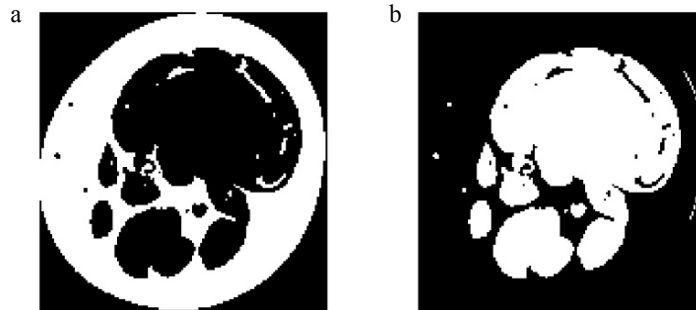


Fig. 3 (a) Threshold output; (b) Fat suppressing mask

T2 weighted image has high signals on fat and water. By overlaying the fat suppressing mask on T2 image, fat signals will be removed while water signals on T2 will be maintained. The addition operation between T1 and T2 would produce 'STIR' like image or other fat suppressed image. Fig. 4(a), 4(b) and 4(c) show MRI T1 ROI, T2 ROI and STIR ROI respectively. The image fusion system produces the 'STIR' like image as shown in Fig. 4(d).

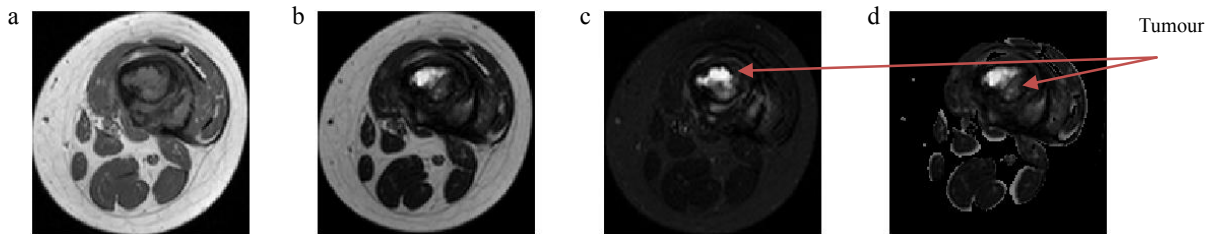


Fig. 4 (a) T1 ROI; (b) T2 ROI; (c) STIR ROI; (d) Fused 'STIR' image

Signal intensity distribution on MRI images could indicate either normal or pathological condition appear in certain tissue. On STIR, there are three signal intensity distribution commonly used to interpret the pathological condition; the high signal region is pathological tissues; intermediate signal is muscle; no signal for bone marrow and fat [3]. The high signal in STIR image is important as shown in Figure 4(c) because it indicates the presence of abnormal fluids such as edema (swelling), necrotic (dead tissue) and viable tumour.

For image quality measurement, the high signal is extracted from both STIR ROI and fused 'STIR' image by using fuzzy C-means algorithm. This is because the high signal is the pathological tissue indicator in STIR image. By using Fuzzy C-Means (FCM), the signal intensity of MRI STIR and fused 'STIR' image is divided into three clusters. MRI STIR image becomes the ground truth (reference image). The high signal intensity of three clusters of MRI STIR is then compared with the high signal intensity of three clusters of fused 'STIR' image.

Mean square error (MSE) and Structural Similarity Index (SSIM) are used to compare signal quality and fidelity between MRI STIR and fused 'STIR' image. MSE is one of the most common and widely used signal fidelity measures. The MSE measures are to compare two signals by providing the level of errors between them. The mathematical equation of MSE is given by the Equation 2 [22, 23];

$$MSE(x, y) = \frac{1}{N} \sum_{i=1}^N (x_i - y_i)^2 \quad (2)$$

where x is the MRI STIR image and y is the fused 'STIR' image; N is the number of signal samples; x_i and y_i are the values of the i th samples in x and y , respectively.

Peak signal-to-noise ratio (PSNR) is the ratio between the maximum possible power of a signal and the power of corrupting noise that affects the fidelity of its representation. The PSNR measure is given by Equation 3 [22, 23];

$$PSNR = 10 \log_{10} \frac{L^2}{MSE} \quad (3)$$

where L is the dynamic range of allowable image pixel intensities.

SSIM is another image fidelity measurement, it measures the similarity based on three elements which are luminance, contrast and structure between two images. The SSIM index is given by Equation 4 [22, 23];

$$S(x, y) = l(x, y) \cdot c(x, y) \cdot s(x, y) = \left(\frac{2\mu_x\mu_y + C_1}{\mu_x^2 + \mu_y^2 + C_1} \right) \cdot \left(\frac{2\sigma_x\sigma_y + C_2}{\sigma_x^2 + \sigma_y^2 + C_2} \right) \cdot \left(\frac{\sigma_{xy} + C_3}{\sigma_x\sigma_y + C_3} \right) \quad (4)$$

where μ_x is the average of MRI STIR image; μ_y is the average of fused 'STIR' image; σ_x is the variance of MRI STIR image; σ_y is the variance of fused 'STIR' image; σ_{xy} is the covariance of MRI STIR image and fused 'STIR' image; $c_1=(k_1L)^2$, $c_2=(k_2L)^2$ two variables to stabilize the division with weak denominator; L the dynamic range of the pixel-values; $k_1=0.01$ and $k_2=0.03$ by default. The SSIM score returns 1 if two images are identical.

Besides MSE and SSIM, Pearson correlation coefficient was calculated to determine the high signal intensity relationship between the MRI STIR and the fused 'STIR' image. Equation 5 shows the formula for Pearson correlation coefficient;

$$\rho = \frac{\sum_{i=1}^n (x_i - \bar{x})(y_i - \bar{y})}{(n-1)s_x s_y} \quad (5)$$

where x is MRI STIR image and y is fused 'STIR' image; \bar{x} is sample mean for x ; s_x is standard deviation for x ; \bar{y} is sample mean for y ; s_y is standard deviation for y and n is column length. The Pearson correlation coefficient is close to 1 if there is a strong high signal intensity relationship between MRI STIR and fused 'STIR' image.

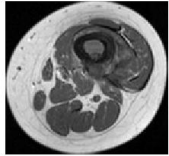
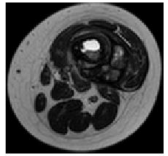
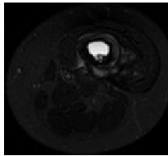
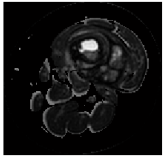
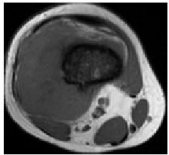
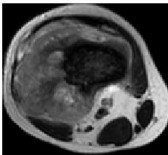
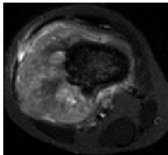
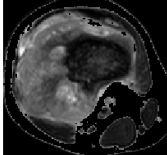
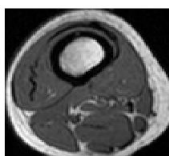
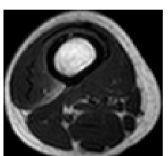
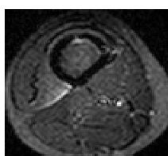
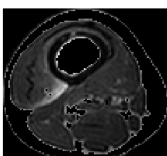
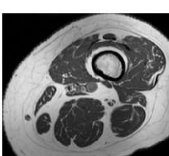
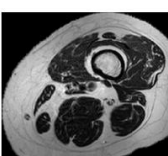
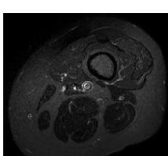
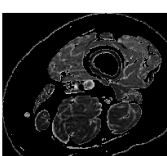
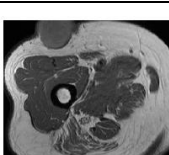
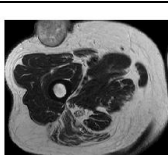
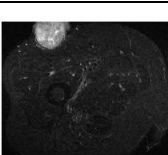
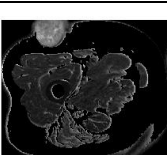
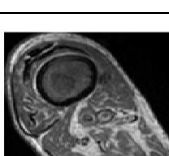

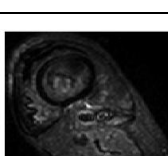

4. Experimental results and discussion

The framework of image fusion system described in Fig. 1 is implemented and tested on nine patients of total 312 slices with different thigh diseases from Hospital Universiti Sains Malaysia (HUSM), Kubang Kerian, Kelantan, Malaysia. The images are in Digital Imaging and Communications in Medicine (DICOM) gray scale format. The dynamic range for the images are 16 bits pixel intensities. The pixel intensities of MR images are represented by 16 bit integer. There are four different image sizes on the tested data which are 224 x 224, 240 x 240, 256 x 256 and 512 x 512. Three MRI machines used have different magnetic power strength. There are two different MRI machines with 1 Tesla and one MRI machine with 3 Tesla respectively. The information about each patient is summarized as in Table 1.

Table 1 Summary of tested MRI images

Patient	Image size	slices	MRI magnetic power (Tesla)	Diagnosis disease
1	224 x 224	32	3	Osteosarcoma
2	224 x 224	27	3	Osteosarcoma – preoperative chemotherapy
3	224 x 224	36	3	Osteosarcoma – post chemotherapy
4	256 x 256	26	3	Giant cell tumour, malignant transformation
5	512 x 512	20	1	Nerve tumour
6	224 x 224	37	3	Malignant fibrous histiocytoma
7	240 x 240	31	3	Femoral benign bone lesion. Giant cell tumour
8	224 x 224	60	3	Popliteal arteries
9	512 x 512	43	1	Aggressive soft tissue tumour

Fig. 5 shows nine resultant images from nine patients. The MSE and SSIM score show that there is high similarity between MRI STIR and fused 'STIR' image. As shown in Fig. 5, the fused 'STIR' image has higher SNR if compared to the MRI STIR image. In the fused image, the structure of muscle is still visible when compared to the MRI STIR.

Image/ MSE, SSIM, Speed	T1 ROI	T2 ROI	STIR ROI (Ground truth)	Fused 'STIR'
Image 1 MSE = 0.0401 PSNR = 110.2955 SSIM = 0.9974 Speed = 4.6606 sec				
Image 2 MSE = 0.0887 PSNR = 106.8527 SSIM = 0.9947 Speed = 5.0896 sec				
Image 3 MSE = 0.2975 PSNR = 101.595 SSIM = 0.9751 Speed = 3.6421 sec				
Image 4 MSE = 0.2112 PSNR = 103.0832 SSIM = 0.9821 Speed = 6.9123 sec				
Image 5 MSE = 0.0794 PSNR = 107.3288 SSIM = 0.9945 Speed = 20.9564 sec				
Image 6 MSE = 0.1667 PSNR = 104.1101 SSIM = 0.9895 Speed = 4.5616 sec				

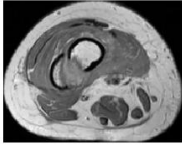
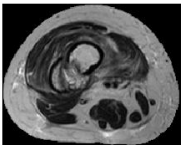
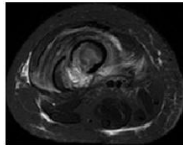
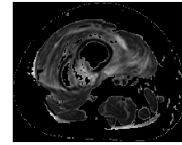
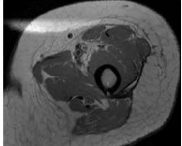
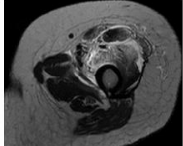
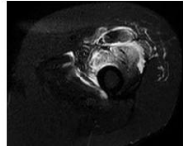
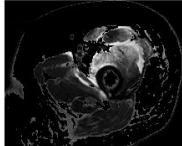
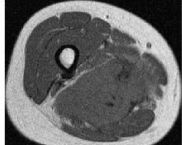
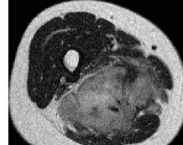
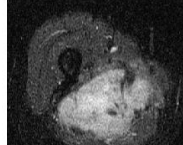
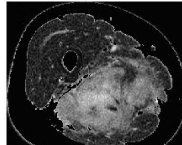
<p>Image 7 MSE = 0.1031 PSNR = 106.1966 SSIM = 0.9943 Speed = 5.388 sec</p>				
<p>Image 8 MSE = 0.0387 PSNR = 110.4475 SSIM = 0.997 Speed = 8.0746 sec</p>				
<p>Image 9 MSE = 0.0803 PSNR = 107.2831 SSIM = 0.9945 Speed = 11.0955 sec</p>				

Fig. 5 Comparison between resultant fused ‘STIR’ image and STIR ROI (as ground truth)

Besides, image fusion system is able to remove the fat tissue effectively. The MSE value for image 3 (0.2975), 4 (0.2112) and 6 (0.1667) are high. This is because the fat tissue is completely removed in the fused ‘STIR’ image. However, due to the imperfectness of MRI machine, the fat tissue is not completely removed. However, the MSE values for others images are satisfactory which are between 0.0387 to 0.1031.

Fig. 5 shows that the PSNR values for the nine images are relatively high which are between 103.0832 to 110.4475. It shows that the signal over the corrupting noise is high. Besides, overall the SSIM score is high which are between 0.9943 to 0.9974. The SSIM score obtained are very close to 1 where 1 indicates the two images are identical.

Pearson correlation coefficient was carried out to measure the relationship between the high signal intensity between MRI STIR and the fused ‘STIR’ image by using Minitab 17. Fig. 6 shows the scatter plot of high intensity signals of MRI STIR versus fused ‘STIR’ images. The Pearson correlation coefficient obtained is 0.696 with p-value 0.000.

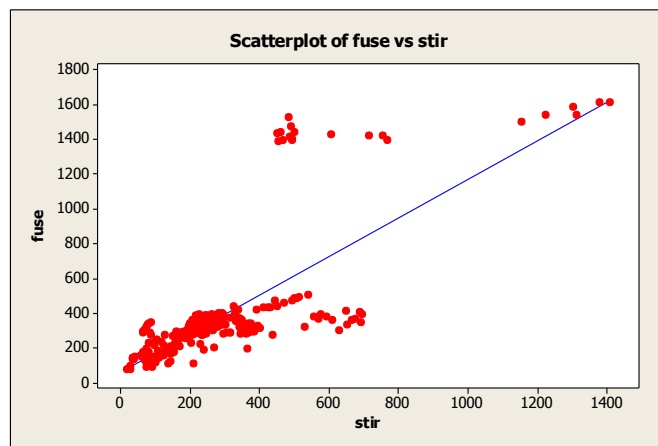


Fig. 6 Scatter plot of high intensity signal of MRI STIR versus fused ‘STIR’ image

The summary of the overall results from all patients which contain 312 slices are shown in Table 2.

Table 2 Overall results for average of MSE, SSIM, Pearson correlation coefficient and P-value

MSE	0.12
PSNR	106.9173
SSIM	0.989971
Pearson correlation coefficient	0.696
P-value	0.000

As shown in Table 2, quantitative analysis from nine patients which contain 312 slices show that MSE is small (0.12). MSE show that the difference or error between STIR and fused STIR image is small. PSNR value is high (106.9173) which indicate that the signal to corrupting noise is high. The SSIM score is being close to 1 (0.989971) shows that the STIR and fused STIR image are highly similar. The overall performance of the image fusion system is statistically significant and the MRI STIR image has good correlation (0.696) with the fused 'STIR' image.

The image fusion system has speedy process as compared to MRI scanning (which can take up to 90 minutes or more depending on the number of weighted images required). The average processing time of the image fusion system for 9 patients are 7.811021 minutes per patient and 7.947 second per slice. The speed of the process depends on the size of the image and the number of slices. A bigger image requires longer time and otherwise. All the experiments are performed on an Intel Core i5-4210U, 2.40GHz processor with 8GB RAM.

5. Conclusion

STIR is an important fat suppressed imaging whereby the fat signal is suppressed. The fat suppression will enhance the contrast of tissues to improve visual inspection during diagnosis. Without fat signals, the appearance of suspected abnormal fluids will be enhanced, making it easier to identify pathological characteristic. Unfortunately, STIR images have inherently lower SNR than other images. This can cause missed diagnoses, missed lesions or over-interpretation of noise as lesions. Because of this, an alternative sequence produced by the image fusion system is proposed to assist specialists in interpreting the STIR image from another point of view. In MRI, STIR uses time delay T1 to nullify longitudinal magnetisation. This is to suppress the fat signals from tissues and increase the echo time (TE) so that another sequence called T2 will increase the contrast between tissues. The image fusion system imitates the MRI machine to produce fused 'STIR' or any other fat suppressed image. A fat suppressing mask which is the inverse of thresholded output is created to mimic the MRI machine to remove the fat tissue. The fused 'STIR' image is produced by overlaying the fat suppressed mask on the T2 to perform the addition operation between T1 and T2. The overall results of 312 slices of image quality measurement analysis shows that the fused 'STIR' image has high similarity with MRI STIR and low MSE. The fused 'STIR' image could remove fat signal effectively and improve the SNR. Besides, image fusion system's performance is statistically significant and the MRI STIR image has good correlation (0.696) with the fused 'STIR' image. On the other hand, the contrast of fused 'STIR' image is higher than the MRI STIR image. Another advantage of image fusion system is that the fused 'STIR' image does not require long processing time as compared to MRI scanning.

Acknowledgements

The authors gratefully acknowledge the valuable comments by the anonymous reviewers and the sponsorship in Ph.D. candidate from the Ministry of Higher Education, Malaysia.

References

- [1] J. K. T. Lee, S. S. Sagel, R. J. Stanley, and J. P. Heiken, "Computered Body Tomography with MRI Correlation," *Lippincott Williams & Wilkins*, vol. 1, 2006.
- [2] O. Tokuda, Y. Harada, and N. Matsunaga, "MRI of Soft-Tissue Tumors: Fast STIR Sequence as Substitute for T1-Weighted Fat-Suppressed Contrast-Enhanced Spin-Echo Sequence," *American Journal of*

- Roentgenology*, vol. 193, pp. 1607-1614, 2009/12/01 2009.
- [3] E. M. Delfaut, J. Beltran, G. Johnson, J. Rousseau, X. Marchandise, and A. Cotten, "Fat Suppression in MR Imaging : Techniques and Pitfalls," *Radiographics*, vol. 19, pp. 373-382, 1999.
 - [4] G. Krinsky, N. M. Rofsky, and J. C. Weinreb, "Nonspecificity of short inversion time inversion recovery (STIR) as a technique of fat suppression: pitfalls in image interpretation," *AJR. American journal of roentgenology*, vol. 166, pp. 523-526, 1996.
 - [5] D. Weishaupt, J. Froehlich, D. Nanz, V. D. Köchli, K. Pruessmann, and B. Marincek, *How Does MRI Work ? An Introduction to the Physics and Function of Magnetic Resonance Imaging*: Springer, 2008.
 - [6] B. Yao, T.-Q. Li, P. v. Gelderen, K. Shmueli, J. A. de Zwart, and J. H. Duyn, "Susceptibility contrast in high field MRI of human brain as a function of tissue iron content," *Neuroimage*, vol. 44, pp. 1259-1266, 2009.
 - [7] E. Van Reeth, I. W. Tham, C. H. Tan, and C. L. Poh, "Super - resolution in magnetic resonance imaging: A review," *Concepts in Magnetic Resonance Part A*, vol. 40, pp. 306-325, 2012.
 - [8] M. Styner, C. Brechbuhler, G. Szckely, and G. Gerig, "Parametric estimate of intensity inhomogeneities applied to MRI," *Medical Imaging, IEEE Transactions on*, vol. 19, pp. 153-165, 2000.
 - [9] G. Steenkiste, B. Jeurissen, J. Veraart, A. J. den Dekker, P. M. Parizel, D. H. Poot, and J. Sijbers, "Super - resolution reconstruction of diffusion parameters from diffusion - weighted images with different slice orientations," *Magnetic Resonance in Medicine*, 2015.
 - [10] D. H. Poot, B. Jeurissen, Y. Bastiaensen, J. Veraart, W. Van Hecke, P. M. Parizel, and J. Sijbers, "Super - resolution for multislice diffusion tensor imaging," *Magnetic Resonance in Medicine*, vol. 69, pp. 103-113, 2013.
 - [11] G. Gerig, O. Kubler, R. Kikinis, and F. A. Jolesz, "Nonlinear anisotropic filtering of MRI data," *Medical Imaging, IEEE Transactions on*, vol. 11, pp. 221-232, 1992.
 - [12] T. Takahara, Y. Imai, T. Yamashita, S. Yasuda, S. Nasu, and M. Van Cauteren, "Diffusion weighted whole body imaging with background body signal suppression (DWIBS) : technical improvement using free breathing, STIR and high resolution 3D display," *Matrix*, vol. 160, p. 160, 2004.
 - [13] T. Ichikawa, S. M. Erturk, U. Motosugi, H. Sou, H. Iino, T. Araki, and H. Fujii, "High-B-value diffusion-weighted MRI in colorectal cancer," *American Journal of Roentgenology*, vol. 187, pp. 181-184, 2006.
 - [14] T. Ichikawa, S. M. Erturk, U. Motosugi, H. Sou, H. Iino, T. Araki, and H. Fujii, "High-b value diffusion-weighted MRI for detecting pancreatic adenocarcinoma: preliminary results," *American Journal of Roentgenology*, vol. 188, pp. 409-414, 2007.
 - [15] A. Oner, H. Celik, S. Oktar, and T. Tali, "Single breath-hold diffusion-weighted MRI of the liver with parallel imaging: initial experience," *Clinical radiology*, vol. 61, pp. 959-965, 2006.
 - [16] H. Greenspan, G. Oz, N. Kiryati, and S. Peled, "MRI inter-slice reconstruction using super-resolution," *Magnetic Resonance Imaging*, vol. 20, pp. 437-446, 2002.
 - [17] G. N. Holland, P. A. Bottomley, and W. S. Hinshaw, "19F magnetic resonance imaging," *Journal of Magnetic Resonance (1969)*, vol. 28, pp. 133-136, 1977.
 - [18] M. Srinivas, A. Heerschap, E. T. Ahrens, C. G. Figdor, and I. J. M. de Vries, "(19)F MRI for quantitative in vivo cell tracking," *Trends in biotechnology*, vol. 28, pp. 363-370, 2010.
 - [19] F. Schmid, C. Hoeltke, D. Parker, and C. Faber, "Boosting 19F MRI—SNR efficient detection of paramagnetic contrast agents using ultrafast sequences," *Magnetic Resonance in Medicine*, vol. 69, pp. 1056-1062, 2013.
 - [20] D. Taylor and M. Bushell, "The spatial mapping of translational diffusion coefficients by the NMR imaging technique," *Physics in medicine and biology*, vol. 30, p. 345, 1985.
 - [21] R. C. Gonzalez and R. E. Woods, *Digital Image Processing*: Pearson Education International, 2010.
 - [22] Z. Wang, A. C. Bovik, H. R. Sheikh, and E. P. Simoncelli, "Image Quality Assessment : From Error Visibility to Structural Similarity," *Image processing, IEEE transactions on*, vol. 13, pp. 600-612, 2004.
 - [23] Z. Wang and A. C. Bovik, "A universal image quality index," *Signal Processing Letters, IEEE*, vol. 9, pp. 81-84, 2002.